Electronic Spectroscopy of an Isolated Halocarbocation: The Iodomethyl Cation CH_2I^+ and Its Deuterated Isotopomers

Chong Tao, Calvin Mukarakate, Yulia Mishchenko, Danielle Brusse, and Scott A. Reid*

Department of Chemistry, Marquette University, Milwaukee, Wisconsin 53201-1881

Received: June 25, 2007; In Final Form: August 2, 2007

Building upon our recent observation of the gas-phase electronic spectrum of the iodomethyl cation (CH_2I^+), we report an extensive study of the electronic spectroscopy of CH_2I^+ and its deuterated isotopomers $CHDI^+$ and CD_2I^+ using a combination of fluorescence excitation and single vibronic level (SVL) emission spectroscopies. The spectra were measured in the gas phase under jet-cooled conditions using a pulsed discharge source. Fluorescence excitation spectra reveal a dominant progression in ν_3 (C−I stretch), the frequency of which is markedly smaller in the upper state. Rotational analysis shows that, while the *A* constant is similar in the two states, the excited state has significantly smaller *B* and *C* constants. These results indicate a lengthening of the C−I bond upon electronic excitation, consistent with calculations which show that this transition is analogous to the well-known $\pi-\pi^*$ transition in the isoelectronic substituted formaldehydes. SVL emission spectra show progressions involving four of the six vibrational modes; only the C−H(D) stretching modes remain unobserved. The vibrational parameters determined from a Dunham expansion fit of the ground state vibrational term energies are in excellent agreement with the predictions of density functional theory (DFT) calculations. A normal-mode analysis was completed to derive a harmonic force field for the ground state, where resonance delocalization of the positive charge leads to partial double bond character, $H_2C^+-I \leftrightarrow H_2C{=}I^+$, giving rise to a C−I stretching frequency significantly larger than that of the iodomethyl radical.

Introduction

Carbocations are among the most important of reactive intermediates,[1] yet have received less attention from gas-phase spectroscopists than other important families of reactive intermediates such as radicals or carbenes. This is not due to a lack of interest, but rather due to difficulties in cleanly preparing these species in the number densities necessary for spectroscopic interrogation. Recently, we observed the first gas-phase electronic spectrum of a halocarbocation, CH_2I^+, produced from CH_2I_2 using a pulsed discharge source.[2] Both excitation and emission spectra were obtained; the latter showed progressions involving two modes, assigned to the a_1 fundamentals ν_2 (CH_2 scissor) and ν_3 (C−I stretch) based on a comparison with density functional theory (DFT) calculations. The assignments were supported by measuring the corresponding spectrum of the d_2-isotopomer, which gave isotopic shifts that were in good agreement with theoretical expectations.

The derived ground state C−I stretching frequency of the iodomethyl cation is significantly larger than that of the iodomethyl radical (611 cm^{-1}),[3] the $CH_2I_2^+$ cation (∼520, 550 cm^{-1}),[4] or other molecules containing C−I single bonds (e.g., CH_3I, 533 cm^{-1}).[5] Moreover, the calculated C−I bond length of CH_2I^+ is almost 0.1 Å shorter than that of CI_3^+.[6] These unusual features were also noted in a computational study of the bromomethyl radical and cation,[7] where a 160 cm^{-1} increase in the C−Br stretching frequency was predicted upon ionization. This increase in frequency, and concomitant decrease in bond length, was attributed to a decrease in repulsion between the C and Br atoms upon ionization.[7] Alternatively, these effects can be viewed as arising via back-donation from the halogen,[6,8] leading to resonance delocalization of the positive charge and partial double bond character: $H_2C^+-I \leftrightarrow H_2C{=}I^+$.

The wavelength of the observed visible system is near that (∼570 nm) of the photoproduct(s) observed following excitation of CH_2I_2 in the condensed phase by ultraviolet radiation,[9−12] pulsed radiolysis,[13,14] or direct photoionization.[15] While resonance Raman studies suggest that both $CH_2I_2^+$ and isodiiodomethane (CH_2I-I) contribute to this band system,[4] it has also been noted that the charge distribution of the CH_2I moiety in isodiiodomethane is similar to that of CH_2I^+.[16] Thus, study of the isolated iodomethyl cation can give insights into the structure of isodiiodomethane. This is important, considering that the ultraviolet photochemistry of diiodomethane has long been used in cyclopropanation reactions with olefins,[17,18] and recent studies have demonstrated the important role of isodiiodomethane in this process.[19] Note that, while the iodomethyl cation also readily reacts with olefins, the product is a stable carbocation.[19,20]

Several recent studies have demonstrated a role for halocarbocations in important gas-phase reactions, providing additional motivation for examining the spectroscopy of the isolated ions. For example, a study of the ionic reactivity of ozone with halocarbocations found a new reaction pathway leading to the extrusion of carbon monoxide, which has implications for atmospheric chemistry.[21] Acting as strong Lewis acids, these species are found to undergo a wide variety of reactions including formation of adducts with N- and O-containing molecules,[22] functionalization of aromatic molecules,[23] and metathesis reactions.[24] In this paper, we present the full results of our spectroscopic analysis of the isolated iodomethyl cation,

* Corresponding author. Email: scott.reid@mu.edu.

10.1021/jp0749322 CCC: $37.00
Published on Web 09/22/2007

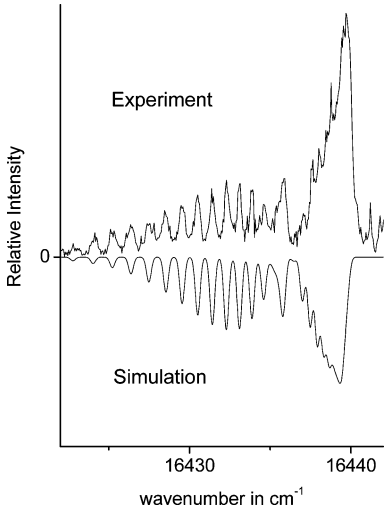

Figure 1. Experimental (top) and simulated fluorescence excitation spectra of the 2_0^1 band of CH_2I^+. The simulation is based on the rotational constants given in the text and assumed a rotational temperature of 20 K.

which have been extended to the singly deuterated isotopomer. Experimental data from fluorescence excitation and single vibronic level emission spectroscopy are combined with density functional theory (DFT) calculations, yielding new insights into the electronic structure of this prototypical carbocation.

Experimental Procedures

The apparatus, pulsed discharge nozzle, and data acquisition procedures have been described in earlier studies.[2,25] The carbocations CH_2I^+, $CHDI^+$, and CD_2I^+ were produced using a pulsed electrical discharge through a ~1−2% mixture of the corresponding diiodomethane (CH_2I_2, $CHDI_2$, or CD_2I_2) seeded in high-purity He. The precursor was kept in a homemade stainless steel bubbler, through which pure He gas was passed at a pressure of 2−4 bar. The discharge pulse width fully encompassed the gas pulse from the nozzle, and the discharge was initiated by a +1 kV pulse of ~700 μs duration, through a current limiting 10 kΩ ballast resistor. The timing of laser, nozzle, and discharge firing was controlled by a digital delay generator (Stanford Research Systems DG535), which generated a variable width gate pulse for the high voltage pulser (Directed Energy GRX-1.5K-E). The laser system consisted of an etalon narrowed dye laser (Lambda-Physik Scanmate 2E) pumped by the second or third harmonic (532 or 355 nm) of a Nd:YAG laser (Continuum NY-61). The laser beam was not focused, and typical pulse energies were ~1−2 mJ in a ~3 mm diameter beam.

A mutually orthogonal geometry of laser, molecular beam, and detector was used, where the laser beam crossed the molecular beam at a distance of ~1 cm downstream. Fluorescence was collected and collimated by a 2 in. diameter, *f*/2.4 plano-convex lens, and focused into the spectrograph using a *f*-matching *f*/3.0 plano-convex lens, also 2 in. in diameter. Insertion of an aluminum mirror into the beam path at 45° allowed collection of the total fluorescence, which was filtered via a long-pass cutoff filter (Corion or Edmund Scientific) prior to striking a photomultiplier tube detector (Oriel) held at typically −700 V. Fluorescence excitation spectra were obtaining by monitoring the total fluorescence as the laser was scanned in typical steps of 0.002 nm; 20−30 laser shots were averaged at each step in wavelength. In acquiring emission spectra, the fluorescence signal was first optimized on the band of interest,

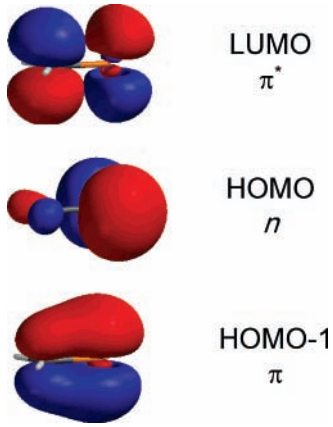

Figure 2. Calculated electron density maps for the two highest occupied molecular orbitals and lowest unoccupied orbital in CH_2I^+. The calculations are described in the text.

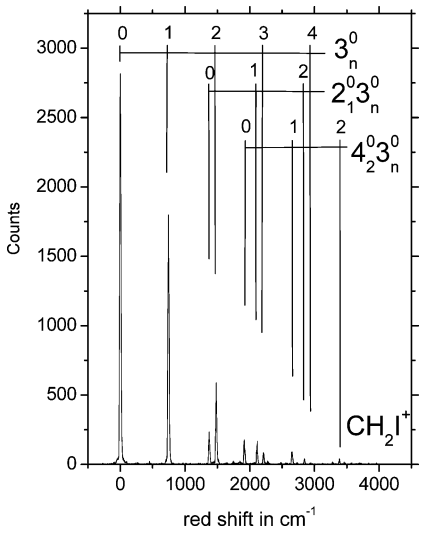

Figure 3. Single vibronic level emission spectrum of CH_2I^+ from the origin band of the visible system. Assignments are noted. The *x*-axis labels the shift in frequency from the excitation line, and thus the vibrational energy in the ground state.

and the mirror subsequently removed to allow fluorescence to enter the spectrograph (Action SR303i with ISTAR CCD). A second removable mirror assembly was used to direct the output of an Fe:Ne hollow cathode lamp into the spectrograph for wavelength calibration; these spectra were typically obtained immediately after the emission spectra and were acquired with a slit width of 10 μm and 500 shot accumulation. Background spectra were obtained with the laser blocked to check for emission lines from species in the discharge.

The emission spectra were acquired in photon counting mode (20 000 shot typical accumulation) with a typical slit width of 100 μm, using a 600 lines/mm grating blazed at 500 nm. The integration gate (typically 4−8 μs) was set to fully encompass the fluorescence decay of the emitting level under our experimental conditions, and the spectrograph was operated in a "step and glue" mode, where the grating was sequentially stepped and spectra were recorded at each grating position in order to cover the entire spectral region of interest. Spectra were calibrated in each range by first fitting the Ne I emission lines to a Gaussian line shape function, using Origin 7.5 software. The observed positions were then compared against the known values,[26] and the deviations were fit to a second-order polynomial to obtain a calibration curve which was applied to the

TABLE 1: Vibrational Term Energies (in cm^{-1}) for the Ground State of CH_2I^+ and Its Deuterated Isotopomers Derived from SVL Emission Spectra[a]

assignment	CH_2I^+	o. − c.[b]	CD_2I^+	o. − c.	$CHDI^+$	o. − c.
2^1	1375[c]	0	1043	0	1243	0
2^2	2732	1	2064	0		
2^13^1	2114	0	1727	−1	1915	0
2^13^2	2846	0	2410	0	2584	0
2^13^3	3571	0	3086	−2		
2^13^4			3760	−1		
2^23^1	3463	−1	2748	2		
2^23^2			3425	1		
2^14^2	3282	0	2529	1		
2^24^2			3539	−2		
3^1	746	1	689	0	677	0
3^2	1482	−1	1375	0	1349	−1
3^3	2215	0	2056	0	2023	4
3^4	2941	1	2736	2	2681	−4
3^5	3658	0			3350	2
3^14^2	2655	0	2179	−1	2395	1
3^24^2	3387	0	2861	−2	3065	0
3^34^2	4112	0				
3^16^1					1450	1
3^26^1					2118	0
3^16^2	2483	0	2010	0	2214	1
3^36^1					2784	−2
3^16^3					2968	−1
4^2	1918	0	1494	1	1720	0
6^1					772	−2
6^2	1747	0	1328	0	1542	1
$2^13^14^2$	4015	0	3212	2		
$2^13^24^2$			3891	2		

[a] Assignments and deviations from a Dunham expansion fit are given. [b] Observed − calculated. [c] Estimated uncertainty in term energies is ±2 cm^{-1}.

corresponding emission spectrum. Bands in the emission spectra were also fit to a Gaussian line shape function.

The precursors CH_2I_2 (99% stated purity) and CD_2I_2 (99 atom % D) were obtained from Sigma-Aldrich Chemical Co. and used without further purification. The $CHDI_2$ precursor was synthesized using a literature preparation.[27]

Results and Discussion

A. Fluorescence Excitation Spectra. Low resolution survey fluorescence excitation spectra of CH_2I^+ revealed several bands in the region extending from the origin at 15 185 cm^{-1} to ~16 600 cm^{-1}, where overlap with the spectrum of I_2 generated in the discharge becomes severe. Based upon single vibronic level emission spectroscopy, described in detail below, these are cold bands originating from the vibrationless level of the $\tilde{X}^1A_1$ state. The three strongest bands (at ~15 181, 15 748, and 16 306 cm^{-1}) were assigned to a progression in the C−I stretch (ω_3'), i.e., 0_0^0, 3_0^1, and 3_0^2. A fit of the data to the expression

$$G(v) = T_{00} + v\omega_3' + v^2x_{33}' \quad (1)$$

yielded T_{00} = 15 180.7 cm^{-1}, ω_3' = 571.3 cm^{-1}, and x_{33}' = −4.2 cm^{-1}. In addition, a weaker band observed at 16 428.7 cm^{-1} was assigned to 2_0^1, giving an excited state anharmonic frequency for the CH_2 scissor mode (ν_2') of 1248.1 cm^{-1}.

Similar progressions were observed in the spectra of the deuterated isotopomers. For $CHDI^+$, analysis yielded T_{00} = 15 244.0 cm^{-1}, ω_3' = 535.7 cm^{-1}, and x_{33}' = −0.7 cm^{-1}. For CD_2I^+, the values were T_{00} = 15 289.4 cm^{-1}, ω_3' = 545.0 cm^{-1}, x_{33}' = −4.6 cm^{-1}, and ν_2' = 1109.0 cm^{-1}. The trend in ω_3' for the three isotopomers mirrors that observed in the ground state, as described below. However, for all three isotopomers a significant reduction in the C−I stretching frequency is observed upon electronic excitation. As noted above, the unusually large C−I stretching frequency in the ground state (~750 cm^{-1} for CH_2I^+) is consistent with partial double bond character, reflecting resonance delocalization of the positive charge: $H_2C^+-I \leftrightarrow H_2C{=}I^+$. In contrast, the excited state frequency is characteristic of a single C−I bond, lying intermediate between those of the iodomethyl radical (611 cm^{-1})[3] and CH_3I (533 cm^{-1}).[5]

The structural changes upon electronic excitation apparent from the vibrational analysis were confirmed by subsequent rotational analysis. In our preliminary report,[2] a simulation of the CH_2I^+ origin band was carried out using the calculated rotational constants of the $\tilde{X}^1A_1$ state, including the proper nuclei spin weighting and assuming singlet multiplicity for both states. The simulation was consistent with an A-type rotational contour, and thus an excited state of A_1 symmetry. In this work, we extended the rotational analysis to other bands in this system, focusing particularly on the 2_0^1 band of CH_2I^+ (Figure 1), the best resolved of the bands. Due to the similarity in *A* rotational constants for the two electronic states of this near-prolate symmetric top, the spectrum contains overlapping contributions from different K_a components under *a*-type selection rules (ΔJ = 0, ±1; ΔK_a = 0; ΔK_c = ±1). At our rotational temperature of ~20 K, the most intense transitions originate from K_a'' = 0 and 1. Note that the asymmetry splitting (i.e., *K*-type doubling) for K_a = 1 is not resolved, even at the highest *J*. Thus, in fitting the observed transitions the same frequency was assigned to a given $^qP_0(J)$ and $^qP_1(J)$ transition, and the upper state term energy and rotational constants (A', B', and C') were varied, with the ground state rotational constants fixed at their ab initio

TABLE 2: Comparison of Calculated Vibrational Parameters for Isotopomers of CH_2I^+ with Those Determined from the Dunham Expansion Fits

parameter	Dunham fit (CH_2I^+)	DFT[a]	Dunham fit (CD_2I^+)	DFT	Dunham fit ($CHDI^+$)	DFT
ω_1		3117		2254		2332
ω_2	1400.3(17)	1424	1067.9(30)	1075	1265.5(35)[b]	1287
ω_3	758.6(7)	753	698.1(17)	695	684.2(30)	688
ω_4	963.1(6)[b]	1017	749.2(11)[b]	793	860.5(18)[b]	914
ω_5		3255		2431		3187
ω_6	875.6(6)[b]	899	665.6(15)[b]	671	783.3(33)	791
x_{22}	−9.7(6)		−10.6(9)		−10.2[c]	
x_{23}	−6.4(4)		−3.8(5)		−4.2(22)	
x_{24}	−5.1(5)		−4.1(6)		0.0[c]	
x_{33}	−3.3(1)		−2.1(3)		−1.8(4)	
x_{34}	−3.4(2)		−1.3(5)		−1.1(11)	
x_{36}	−4.3(6)		−3.7(14)		−2.7(9)	
x_{44}	0.0[c]		0.0[c]		0.0[c]	
x_{66}	0.0[c]		0.0[c]		−3.8(9)	

[a] Calculated at the B3LYP/6-311G** level. [b] Anharmonic frequency. [c] Fixed in the fit.

(B3LYP/6-311G**) values (in cm^{-1}): $A'' = 9.417$, $B'' = 0.3177$, and $C'' = 0.3074$. Fitting 33 levels to a standard deviation of 0.03 cm^{-1}, the derived upper state rotational constants are as follows (in cm^{-1}): $A' = 9.393(36)$, $B' = 0.2948(7)$, and $C' = 0.2822(7)$.

Our decision to fix the ground state rotational constants in the fit, while necessitated by the limited resolution of our spectra, does introduce a degree of uncertainty in the derived upper state constants. However, we are confident in the qualitative result of this simulation, namely, similar A rotational constants for the two electronic states and a decrease in B and C upon electronic excitation. The magnitude of the decrease in B and C indicates a lengthening of the C−I bond by ∼0.08 Å in the upper state.

Given that the monohalomethyl cations (H_2CX^+; X = F, Cl, Br, I) are isoelectronic with the substituted formaldehydes (H_2CY; Y = O, S, Se, Te), we can obtain further insight into this electronic transition from a comparison with the well-known spectroscopy of the formaldehydes. In addition, we carried out density functional theory (DFT) calculations at the B3LYP/6-311G** level using the Gaussian 98 program package[28] on a personal computer; the iodine basis set was obtained from the EMSL/PNL Basis Set Library.[29] Electron density maps of the two highest occupied molecular orbitals (HOMOs) and lowest unoccupied molecular orbital (LUMO) are shown in Figure 2. The highest occupied molecular orbital (HOMO) is a nonbonding p_y orbital of b_2 symmetry centered on the iodine. In contrast, the LUMO is a π^* orbital (b_1 symmetry) localized on the C−I moiety. A one-electron promotion from HOMO to LUMO gives an A_2 electronic state, which is symmetry forbidden in an electric dipole transition from the ground state; in the formaldehydes this transition is vibronically induced and occurs in the near-infrared (H_2CSe) to near-ultraviolet (H_2CO).[30−32] However, promotion of an electron from the second HOMO to the LUMO, analogous to the well-known formaldehyde $\pi-\pi^*$ transition,[30] gives rise to an A_1 electronic state. Thus, we assign the observed transition as $\tilde{X}^1A_1 \rightarrow \tilde{A}^1A_1$, noting that the multiplicity of the upper state has not been unambiguously established by these experiments.

B. Single Vibronic Level (SVL) Emission Spectra. We obtained emission spectra from most of the observed upper state levels; an example SVL emission spectrum of CH_2I^+ from the origin transition is shown in Figure 3. The various spectra allowed identification of spurious peaks due to the discharge background or collision-induced relaxation in the excited state, and helped clarify the upper state assignments. For CH_2I^+, emission spectra showed a series of progressions originating at 0, 1375, 1748, and 1918 cm^{-1}, built upon one mode with an anharmonic frequency of ∼746 cm^{-1}. As the electronic transition occurs between states of A_1 symmetry, we expect to observe fundamentals of totally symmetric vibrations and even-numbered overtones (or symmetric combinations) of nontotally symmetric vibrations. Calculations at the B3LYP/6-311G** level predict two a_1 fundamentals (ν_2, CH_2 scissor; ν_3, C−I stretch) with frequencies near 1400 and 750 cm^{-1}, respectively, a b_1 fundamental (ν_4, CH_2 wag) near 1000 cm^{-1}, and a b_2 fundamental (ν_6, CH_2 rock) near 900 cm^{-1}. The dominant progressions were thus assigned as 3_n^0, $2_1^0 3_n^0$, $4_2^0 3_n^0$, and $6_2^0 3_n^0$.

These assignments were confirmed by obtaining spectra of the deuterated isotopomers. As expected, the frequency of ν_3 (C−I stretch) was less sensitive to deuterium substitution, while the other modes displayed large deuterium shifts, consistent with their assignment to motions involving the CH_2 moiety. For the *hd*-isotopomer, the reduction in symmetry led to the observation of the fundamental of ν_6, as well as combination bands involving odd quanta of ν_4 and ν_6.

For each isotopomer, we fit the observed $\tilde{X}$ state term energies using a nonlinear least-squares routine to an anharmonic energy function (Dunham expansion) of the form[33]

$$G = \sum_i (\nu_i + 1/2)\,\omega_i + \sum_{j \geq i,i} (\nu_i + 1/2)(\nu_j + 1/2)x_{ij} \quad (2)$$

where ω_i is the harmonic frequency of mode i, x_{ii} is a diagonal anharmonicity constant, and x_{ij} is an off-diagonal or cross-anharmonicity constant. As the fundamentals of ν_4 and ν_6 were not observed for the symmetric isotopomers, the anharmonicity constants x_{44} and x_{66} were set to zero, and the derived

TABLE 3: Results of the Normal-Mode Analysis[a,b]

parameter	experiment (CH_2I^+)	o. − c.[c]	experiment (CD_2I^+)	o. − c.	experiment ($CHDI^+$)	o. − c.
ω_2	1400.3	−8.3	1067.9	2.9	1265.5	−3.4
ω_3	758.6	−1.8	698.1	−0.1	684.2	4.1
ω_4	963.1	−0.8	749.2	−1.2	860.5	−3.0
ω_6	875.6	0.6	665.6	11.0	783.3	−1.7

[a] Derived force field parameters: $f_{33} = 1.270(6)$; $f_{35} = 0.347(13)$; $f_{44} = 0.463(2)$; $f_{34} = f_{45} = 0.0$ (assumed); $f_{55} = 4.303(22)$; $f_{66} = 0.340(1)$. [b] Coordinate notation: 3 = CH_2 scissor; 4 = CH_2 rock; 5 = C−I stretch; 6 = CH_2 out-of-plane bend. [c] Observed − calculated.

frequencies for these two modes represent anharmonic values. For the *hd*-isotopomer x_{66} was determined; however, the constants x_{22}, x_{24}, and x_{44} could not be determined. Since x_{22} was nearly identical for the h_2- and d_2-isotopomers, we fixed x_{22} for the *hd*-isotopomer at the average of the two; x_{24} and x_{44} were fixed at zero. Assignments, term energies, and deviations from the Dunham expansion fit are shown in Table 1, while Table 2 presents the derived Dunham parameters. The fit parameters are compared in Table 2 with the results of DFT calculations at the B3LYP/6-311G** level. Note that the B3LYP functional is quite robust for predicting harmonic vibrational frequencies of both stable and transient molecules.[5,16,25,34] Optimized geometric parameters were $r_{C-H} = 1.087$ Å, $r_{C-I} = 1.963$ Å, $\theta_{HCH} = 120.3°$, and $\theta_{HCI} = 119.9°$. The agreement of experiment and theory is very good for all three isotopomers (Table 2), particularly given the incomplete set of anharmonic constants.

Using the derived harmonic frequencies and ASYM40 program of Hedberg and Mills,[35] a normal-mode analysis was performed. The force field parameters are presented in Table 3.

Conclusions

We have reported studies of the electronic spectroscopy of CH_2I^+ and its deuterated isotopomers $CHDI^+$ and CD_2I^+ using a combination of fluorescence excitation and SVL emission spectroscopies. The fluorescence excitation spectra reveal a progression in ν_3 (C−I stretch), the frequency of which is markedly smaller in the upper state. Rotational analysis shows that while the *A* rotational constant is similar in the two states, the excited state has significantly smaller *B* and *C* constants. These results indicate a significant weakening of the C−I bond upon electronic excitation, consistent with DFT calculations which show that this transition is analogous to the well-known $\pi-\pi^*$ transition in the isoelectronic substituted formaldehydes. SVL emission spectra show progressions involving four of the six vibrational modes; at this point only the C−H(D) stretching modes remain unobserved. The vibrational parameters determined from a Dunham expansion fit of the ground state vibrational term energies are in excellent agreement with DFT predictions. A normal-mode analysis was completed to derive a harmonic force field for the ground state, where resonance delocalization of the positive charge leads to partial double bond character, $H_2C^+-I \leftrightarrow H_2C{=}I^+$, giving rise to a C−I stretching frequency significantly larger than that of the iodomethyl radical. In this regard, the iodomethyl cation is the most stable of the monohalomethyl cations,[6,36] which helps explain why it has been the first observed spectroscopically.

In future work, it is highly desirable to obtain higher resolution, fully rotationally resolved spectra of bands in the visible system, and to examine the analogous system in the other monohalomethyl cations.

Acknowledgment. The National Science Foundation (Grant CHE-0353596) is gratefully acknowledged for support of this research. The authors thank Robert Forner for assistance in data analysis and the DFT calculations.

References and Notes

(1) McClelland, R. A. In *Reactive Intemediate Chemistry*; Moss, R. A., Platz, M. S., Jones, M., Jr., Eds.; Wiley: Hoboken, NJ, 2004; Chapter 1.

(2) Tao, C.; Mukarakate, C.; Reid, S. A. *J. Am. Chem. Soc.* **2006**, *128*, 9320−9321.

(3) Smith, D. W.; Andrews, L. *J. Chem. Phys.* **1973**, *58*, 5222−5229.

(4) Li, Y.-L.; Wang, D.; Leung, K. H.; Phillips, D. L. *J. Phys. Chem. A* **2002**, *106*, 3463−3468.

(5) *NIST Chemistry Webbook*; http://webbook.nist.gov.

(6) Frenking, G.; Fau, S.; Marchand, C. M.; Grützmacher, H. *J. Am. Chem. Soc.* **1997**, *119*, 6648−6655.

(7) Li, Z.; Francisco, J. S. *J. Chem. Phys.* **1999**, *110*, 817−822.

(8) Robbins, A. M.; Jin, P.; Brinck, T.; Murray, J. S.; Politzer, P. *Int. J. Quantum Chem.* **2006**, *106*, 2904−2909.

(9) Simons, J. P.; Tatham, P. E. R. *J. Chem. Soc., A* **1966**, 854−859.

(10) Mohan, H.; Rao, K. N.; Iyer, R. M. *Radiat. Phys. Chem.* **1984**, *23*, 505−508.

(11) Maier, G.; Reisenauer, H. P. *Angew. Chem., Int. Ed. Engl.* **1986**, *25*, 819−822.

(12) Maier, G.; Reisenauer, H. P.; Hu, J.; Schaad, L. J.; Hess, B. A., Jr. *J. Am. Chem. Soc.* **1990**, *112*, 5117−5122.

(13) Mohan, H.; Iyer, R. M. *Radiat. Eff.* **1978**, *39*, 97−101.

(14) Mohan, H.; Moorthy, P. N. *J. Chem. Soc., Perkin Trans. 2* **1990**, 277−282.

(15) Andrews, L.; Prochaska, F. T.; Ault, B. S. *J. Am. Chem. Soc.* **1979**, *101*, 9−15.

(16) Zheng, X.; Phillips, D. L. *J. Phys. Chem. A* **2000**, *104*, 6880−6886.

(17) Blomstrom, D. C.; Herbig, K.; Simmons, H. E. *J. Org. Chem.* **1965**, *30*, 959−964.

(18) Kropp, P. J. *Acc. Chem. Res.* **1984**, *17*, 131−137.

(19) Phillips, D. L.; Fang, W.-H.; Zhang, X. *J. Am. Chem. Soc.* **2001**, *123*, 4197−4203.

(20) Phillips, D. L.; Fang, W.-H. *J. Org. Chem.* **2001**, *66*, 5890−5896.

(21) Cacace, F.; De Petris, G.; Pepi, F.; Rosi, M.; Troiani, A. *Chem.—Eur. J.* **2000**, *6*, 2572−2581.

(22) O'Hair, R.-A. J.; Gronert, S. *Int. J. Mass Spectrom.* **2000**, *195−196*, 303−317.

(23) Sorrihla, A. E. P. M.; Santos, L. S.; Gozzo, F. C.; Sparrapan, R.; Augusti, R.; Eberlin, M. *J. Phys. Chem. A* **2004**, *108*, 7009−7020.

(24) Nguyen, V.; Mayer, P. S.; Morton, T. H. *J. Org. Chem.* **2000**, *65*, 8032−8040.

(25) Deselnicu, M.; Tao, C.; Mukarakate, C.; Reid, S. A. *J. Chem. Phys.* **2006**, *124*, 134302-1−134302-11.

(26) *NIST Atomic Spectra Database*, version 3.0; http://physics.nist.gov/PhysRefData/ASD.

(27) Saljoughian, M.; Morimoto, H.; Williams, P. G.; DeMello, N. *J. Chem. Soc., Chem. Commun.* **1990**, 1652−1653.

(28) Frisch, M. J.; et al. *Gaussian 98*, rev. A.111.4; Gaussian, Inc.: Pittsburgh, PA, 2002.

(29) Basis sets were obtained from the Extensible Computational Chemistry Environment Basis Set Database, version 02/02/06, as developed and distributed by the Molecular Science Computing Facility, Environmental and Molecular Sciences Laboratory, which is part of the Pacific Northwest Laboratory, P. O. Box 999, Richland, WA 99352, and funded by the U.S. Department of Energy.

(30) Clouthier, D. J.; Ramsay, D. A. *Annu. Rev. Phys. Chem.* **1983**, *34*, 31−58.

(31) Clouthier, D. J.; Judge, R. H.; Moule, D. C. *Chem. Phys.* **1987**, *114*, 417−422.

(32) Judge, R. H.; Clouthier, D. J.; Moule, D. C. *J. Chem. Phys.* **1988**, *89*, 1807−1812.

(33) Herzberg, G. *Molecular Spectra and Molecular Structure III. Electronic Spectra of Polyatomic Molecules*; Van Nostrand: New York, 1966.

(34) Scott, A. P.; Radom, L. *J. Phys. Chem.* **1996**, *100*, 16502−16513.

(35) Hedberg, L.; Mills, I. M. *J. Mol. Spectrosc.* **2000**, *203*, 82−95.

(36) Kapp, J.; Schade, C.; El-Nahas, A. M.; Schleyer, P. v. R. *Angew. Chem., Int. Ed. Engl.* **1996**, *35*, 2236−2238.